

See discussions, stats, and author profiles for this publication at: <https://www.researchgate.net/publication/7097137>

# Wetting Transition in Cylindrical Alumina Nanopores with Polymer Melts

ARTICLE *in* NANO LETTERS · JUNE 2006

Impact Factor: 13.59 · DOI: 10.1021/nl060407n · Source: PubMed

---

CITATIONS

165

---

READS

26

6 AUTHORS, INCLUDING:



Jiun-Tai Chen

National Chiao Tung University

58 PUBLICATIONS 1,076 CITATIONS

SEE PROFILE

# Wetting Transition in Cylindrical Alumina Nanopores with Polymer Melts

Mingfu Zhang, Priyanka Dobriyal, Jiun-Tai Chen, and Thomas P. Russell\*

*Department of Polymer Science and Engineering, University of Massachusetts, Amherst, Massachusetts 01003*

Jessica Olmo

*Ludlow High School, Ludlow, Massachusetts 01056*

Aurora Merry

*Salem High School, Salem, New Hampshire 03079*

*Received February 21, 2006*

## ABSTRACT

We report a systematic study of the wetting of cylindrical alumina nanopores with polystyrene melts. A transition from partial to complete wetting was observed with increasing annealing temperature, resulting in the formation of very different one-dimensional polymeric nanostructures (nanorods and nanotubes) within cylindrical alumina nanopores. The wetting transition temperature is dependent on the polymer molecular weight. The large difference in the wetting rate between partial and complete wetting was successfully used to fractionate polymers with different molecular weights.

The wetting of a solid substrate with a liquid has attracted substantial interest<sup>1</sup> because of its various technical applications, including coatings, lubrication, adhesion, painting, and nanoimprinting. Different wetting regimes can be classified according to the spreading coefficient  $S$ , which is defined by<sup>1,2</sup>

$$S = \gamma_{\text{SG}} - \gamma_{\text{SL}} - \gamma \quad (1)$$

where,  $\gamma_{\text{SG}}$ ,  $\gamma_{\text{SL}}$ , and  $\gamma$  represent the solid–gas, solid–liquid, and liquid–gas interfacial tensions, respectively.  $S$  measures the interfacial energy difference between the bare substrate and the substrate covered with a film of liquid. If  $S \geq 0$ , complete wetting will occur and a liquid droplet will spread spontaneously on the solid substrate until a complete coverage of the substrate with a thin liquid film is achieved. If  $S < 0$ , a liquid drop deposited on the solid substrate will spread partially and eventually reach an equilibrium shape with a finite contact angle,  $\theta_c$ , defined by Young's equation:  $\cos \theta_c = (\gamma_{\text{SG}} - \gamma_{\text{SL}})/\gamma$ . Wetting, in the case of a negative spreading coefficient, is called partial wetting.

It is well-known that some “high-energy” solids (characterized by high surface tension), such as glass, metals, metal oxides, and ionic crystals, are wettable by almost all “low-

energy” liquids, including polymer melts. Recently, wetting “high-energy” solid substrates with polymer melts has become a subject of intensive research, due to the novel structures (layering, fingering) that form in the resultant polymer films.<sup>3,4</sup> Two wetting regimes (partial wetting and complete wetting) have been studied. In the complete wetting regime, a very interesting phenomenon has been observed which is the existence of a microscopic precursor film spreading ahead of the macroscopic front of a polymer liquid on solid substrate.<sup>3,5–9</sup> The thickness of the polymer precursor film is typically less than 100 nm, while its spatial extension on a solid substrate can approach the millimeter range within a relatively short period of time. For example, a precursor film of poly(dimethylsiloxane) (PDMS) can extend millimeters on silicon wafer within hours.<sup>3</sup>

Particularly, when nanoporous “high-energy” solid materials are used as wetting templates, polymeric nanostructures can be generated by solidification of polymer melts within the nanopores. For example, alumina membranes possessing cylindrical nanopores that are perpendicular to the macroscopic membrane surface, are ideal templates for the preparation of one-dimensional (1-D) polymeric nanostructures (nanorods and nanotubes) by using polymer melts as wetting liquids.<sup>10,11</sup> After the wetting and subsequent solidification, the resultant polymeric nanostructures can be easily released from the templates simply by dissolving the alumina in mild aqueous acidic or basic solutions.

\* To whom correspondence should be addressed. E-mail: russell@mail.pse.umass.edu. Phone: +1 (413) 577-1516. Fax: +1 (413) 577-1510.

Similar to the case of a flat solid substrate, two wetting regimes (partial wetting and complete wetting) are also observed when nanoporous alumina membranes are wetted by polymer melts. In the partial wetting regime, cylindrical nanopores, which can be regarded as nanosized capillaries, are gradually filled with polymer melts via capillary action. Upon cooling to a temperature lower than the glass transition temperature or the crystallization temperature of the polymer, polymer melts will solidify within the nanopores and polymeric nanorods will be produced. An important signature of capillary action is the presence of a meniscus at the tip of the resultant nanorods, from which the contact angle between the polymer melt and the inner wall of cylindrical nanopore of alumina membrane can be determined. In the complete wetting regime, the precursor film will form and spread on the inner walls of nanopores in alumina membranes. Taking into account the fast spreading of the precursor film on the substrate,<sup>3</sup> complete coverage of the inner wall of cylindrical nanopores with the length of  $\sim 60\text{ }\mu\text{m}$  by a precursor film can be achieved very quickly, as compared to the slow capillary rise of polymer melts within the alumina nanopores in the partial wetting regime.<sup>12</sup> If the diameter of the cylindrical nanopore is larger than two times the thickness of precursor film, hollow nanotubes will be produced upon quenching.

For the wetting of solid substrates by liquids, a temperature ( $T_w$ ) is predicted for a transition from the partial to complete wetting ( $\theta_c(T_w) = 0$ ).<sup>1,13</sup>  $T_w$  is called the wetting transition temperature. To observe  $T_w$ , one needs to investigate the wetting behavior over a broad range of temperatures so that the changes in the interfacial tensions are large enough to change the sign of  $S$ . For volatile liquids on solids, it is practically difficult to study the wetting transition, because high pressure is normally needed to maintain the liquid/vapor equilibrium. Fortunately, for nonvolatile polymer melts on solid substrates, the study of the wetting transition can be carried out at atmospheric pressure or even under vacuum. For most polymers there is a relatively broad temperature range available between the glass transition temperature (or the melting temperature) and the thermal decomposition temperature, which is crucial for the study of the wetting transition. Surprisingly, very few studies about the wetting transition of polymer melts on solid substrates have been reported,<sup>14</sup> though both partial and complete wetting of polymer melts on substrates have been studied intensively. This is most probably due to the technical difficulty in the observation of wetting transition on a flat solid substrate. Fortunately, as a unique wetting template, alumina membranes possessing cylindrical nanopores offer a simple method to study the wetting transition, because the transition from the partial wetting regime to the complete wetting regime (or vice versa) gives rise to the formation of very different polymeric nanostructures (from nanorod to nanotube, or vice versa), which can be easily observed by microscopy techniques. Thus, simply from the resultant polymeric nanostructures, we can determine the wetting mechanism and, thus, measure  $T_w$ .

Recently, wetting nanoporous alumina membranes with polymer melts has become an active area of research due to

its simplicity and versatility in generating 1-D polymeric nanostructures and for the modification of morphologies of block copolymers<sup>12,15–17</sup> and crystalline polymers<sup>18</sup> under the confinement of cylindrical nanopores. Both polymeric nanorods<sup>10,12,15–17</sup> and nanotubes<sup>11,18,19</sup> have been successfully generated by wetting nanoporous alumina membranes with various polymer melts via the two wetting mechanisms described above. In the partial wetting regime, melts of both homopolymers<sup>10</sup> and block copolymers<sup>12,15–17</sup> have been successfully introduced into the nanopores of alumina membranes to generate polymer nanorods. The length (and thus the aspect ratio) of the resultant polymer nanorods can be controlled simply by controlling the annealing time. The packing and the period of the microdomains of diblock copolymers within cylindrical nanopores differed significantly from those observed in the bulk due to the cylindrical nanoconfinement and an incommensurability between the pore geometry and the natural period of diblock copolymer.<sup>12,15–17</sup> In the complete wetting regime, polymeric nanotubes were generated within alumina membranes via the spreading of the precursor film. For example, Steinhart and co-workers have successfully fabricated various polymeric nanotubes by wetting alumina membranes with polymer melts.<sup>11,18,19</sup> It has been found that the wetting of the inner wall of nanopores in alumina membranes by precursor film was a very rapid process (complete coverage could be achieved within half an hour).

Although both polymeric nanorods and nanotubes have been successfully generated by wetting alumina membranes with polymer melts, no systematic study has been conducted so far to investigate the wetting transition, which is crucial for the control of the wetting behavior and thus the formation of tailored polymeric nanostructures. In this paper, we studied the wetting behavior of polystyrene melts using nanoporous alumina membranes as templates by systematically changing the annealing temperature and polymer molecular weight, aiming to find out the wetting transition. For this purpose, polystyrenes with different molecular weights were used to wet alumina membranes under different annealing temperatures. All polystyrenes used in this work were synthesized anionically and have very low polydispersities, so the influence of molecular weight distribution on the wetting behavior could be minimized.

First, a polystyrene with relatively low molecular weight (PS-1, number-average molecular weight ( $M_n$ ) = 30.5 kg/mol, polydispersity index (PDI) = 1.04) was used to wet alumina membranes at different temperatures. At the annealing temperature of 130 °C, which is slightly above the glass transition temperature ( $T_g$ ) of polystyrene, relatively short PS nanorods with the average length of about 5  $\mu\text{m}$  were generated within alumina membranes after 2 h of thermal annealing, as shown in Figure 1a. The center of the nanorod end appears darker than the edge (Figure 1b), suggesting the existence of a meniscus at the tip of the resultant nanorods. This is a signature of the capillary action. The shallow depression in the center of nanorod end indicates that the contact angle ( $\theta_c$ ) at polystyrene/capillary wall interface is quite large, suggesting that, at this relatively low

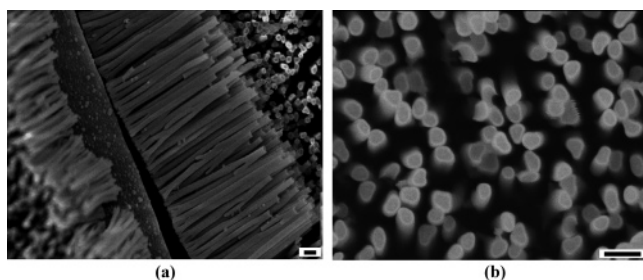


**Figure 1.** SEM images of PS-1 ( $M_n = 30.5$  kg/mol) nanorods generated within alumina membrane after annealing at 130 °C for 2 h: (a) side view (scale bar 500 nm); (b) top view (scale bar 500 nm). The alumina template has been removed by 2 wt % of NaOH aqueous solution.

annealing temperature (130 °C), the wetting of alumina nanopores by polystyrene melts is located in the partial wetting regime, i.e.,  $S < 0$ .

Because of the polydisperse pore size and some structural defects (branching) of nanopores in commercial alumina membranes, the resultant nanorods are not of uniform length (Figure 1a), as one would expect from the theory of capillary action.<sup>20</sup> The rate of the flow of polymer melt in the nanopore can be estimated by<sup>20</sup>

$$dz/dt = R\gamma \cos \theta_c / (4\eta z) \quad (2)$$

where  $t$  is the time,  $z$  the length of the column of polymer melt in the nanopore,  $\eta$  the viscosity of the polymer melt, and  $R$  the hydraulic radius (the ratio between the volume of the liquid in the capillary section and the area of solid/liquid interface;  $R$  is one-half the radius of nanopore). Obviously the rate of capillary rise is dependent on the size of the capillary; thus the pore size distribution of commercial alumina membranes leads to the length distribution of the resultant polystyrene nanorods. From eq 2 we know that filling the cylindrical nanopores in the alumina membranes with polymer melts via the capillary action is very slow due to the small value of  $R$  and the high viscosity of polymer melts. As an example, complete filling of the cylindrical nanopores in the alumina membranes used here (with the average pore size of 200 nm and the length of 60  $\mu\text{m}$ ) with PS-1 melts at 130 °C takes  $\sim 12$  days, based on eq 2 and the results shown in Figure 1a.

When the annealing temperature was raised to 205 °C,  $\sim 100$  °C above the  $T_g$  of polystyrene, very long polystyrene nanotubes were generated, as shown in Figure 2. The length of the resultant polystyrene nanotubes equals to the length of cylindrical nanopores in alumina membranes (60  $\mu\text{m}$ ), indicating the wetting was a rapid process. The generation of polystyrene nanotubes was ascribed to the spreading of the polymeric precursor film on the inner walls of the alumina nanopores.<sup>11</sup> As mentioned above, the precursor film can extend over millimeters on the substrate within hours;<sup>3</sup> thus the walls of alumina nanopores can be completely covered by the precursor film, taking into account the finite length of the nanopores (60  $\mu\text{m}$ ).

Different from the polystyrene nanorods formed at low annealing temperatures, which were separate from each other

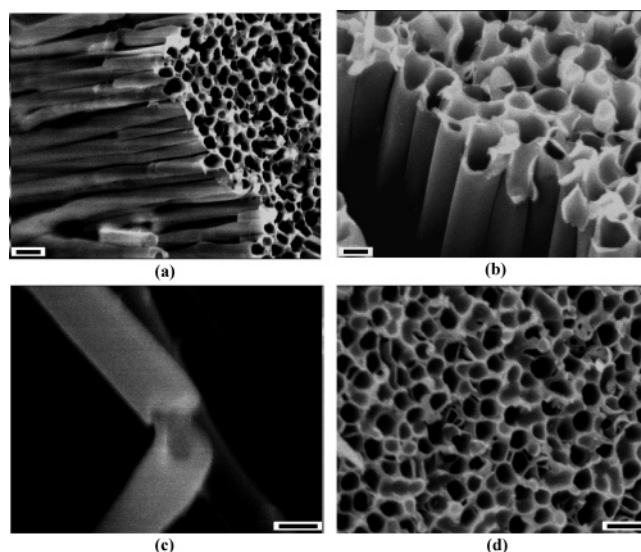


**Figure 2.** SEM images of PS-1 ( $M_n = 30.5$  kg/mol) nanotubes generated within alumina membrane after annealing at 205 °C for 2 h: (a) and (b) side view (scale bar 500 nm in (a) and 200 nm in (b)); (c) a broken nanotube (scale bar 200 nm); and (d) top view (scale bar 500 nm).

at the tip (Figure 1), the nanotubes formed at high temperatures were all held together by a thin surface layer of polystyrene, as shown in Figure 2d. This indicates that the precursor film wet not only the walls of the nanopores but also the free surface of the alumina membrane. In other words, the precursor film wet all available high-energy surfaces within 2 h. Because of the limited wettable surface in the alumina membrane and the fast spreading of precursor film, complete coverage of all wettable surfaces in the alumina membrane by the precursor film was achieved very rapidly. Obviously, the thermodynamic equilibrium state, which corresponds to the complete filling of the nanopores with polystyrene melt, was not reached within the experimental annealing time (2 h), more than likely due to the slow kinetics of the filling of polystyrene nanotubes with polymer melts. Thus, hollow nanotubes were obtained upon thermal quenching.

By careful comparison of the wall thicknesses at different positions along the polystyrene nanotubes (panels b and c of Figure 2), one can see a thickness gradient, with a decreasing thickness from the bottom to the tip. This is in good agreement with that observed in the precursor film of poly(dimethylsiloxane) (PDMS) on a silicon wafer.<sup>3</sup> On high-energy surfaces, like a silicon wafer, the polymer precursor film consists of several monolayers and shows a thickness gradient toward the edge of precursor film.<sup>3</sup>

Since the size of the nanopores in the alumina membranes is much smaller than the capillary length  $\kappa^{-1}$  ( $\kappa^{-1} = \gamma^{0.5} / (\rho g)^{0.5}$ , where  $\gamma$  and  $\rho$  are the surface tension and the density of polymer melt, respectively), which is in the millimeter range for polystyrene melts, gravitational effect is negligible during wetting. When the alumina membranes were placed either above or under the polymer films during the thermal annealing, identical polystyrene nanostructures were obtained.



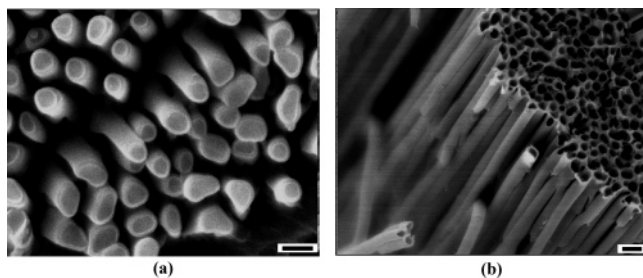


**Figure 3.** SEM images of PS-2 ( $M_n = 83.3$  kg/mol) nanostructures generated within alumina membranes: (a) nanorods obtained after annealing at 125 °C for 2 h (scale bar 500 nm); (b) nanotubes obtained after annealing at 192 °C for 2 h (scale bar 500 nm).

From the results described above, it is obvious that there is a transition from the partial wetting to complete wetting when the annealing temperature was raised from 130 to 205 °C, for the wetting of commercial alumina membranes with PS-1 melts. An increase in  $S$  (from negative to positive) upon heating is responsible for this wetting transition. The temperature dependence of  $S$  should be related to the different temperature coefficients of the three interfacial tensions shown in eq 1. Consequently, there must be a transition temperature,  $T_w$ , between partial and complete wetting, i.e.,  $\theta_c(T_w) = 0$ . For PS-1,  $T_w$  is between 130 and 205 °C.

When a polystyrene with higher molecular weight (PS-2,  $M_n = 83.3$  kg/mol, PDI = 1.02) was used, the wetting behavior was observed to be very similar to that of PS-1. As shown in Figure 3, at relatively low temperature (125 °C), very short nanorods were obtained after 2 h of thermal annealing; while at high annealing temperature (192 °C), long nanotubes with length equal to that of alumina nanopores were generated. Again, at high annealing temperatures a surface wetting layer was observed which held the resultant nanotubes together, preventing the long nanotubes from collapsing.

Transmission electron microscopy (TEM) was used to investigate the polystyrene nanotubes formed at high annealing temperatures. Figure 4 showed some typical TEM images of the PS-2 nanotubes. Two sample preparation methods, i.e., microtoming and ultrasonication, were used. Figure 4a shows a TEM image (of a sample prepared via microtoming) where one can see the hollow tubular structure of polystyrene nanotubes. The walls of the nanotubes in this sample are quite thin, since the observed section was cut from the top part of the long nanotubes, as those shown in Figure 2b. Alternatively, the TEM samples can also be prepared via ultrasonication. Figure 4b shows a typical TEM image of the sample prepared via ultrasonication. Again, the hollow tubular structure is observed, as revealed by the brighter middle part and slightly darker edge. In comparison with Figure 4a, the nanotube shown in Figure 4b has a thicker wall. It has to be noted that during the TEM measurements of the samples from ultrasonication we observed some thin pieces of polystyrene, which probably came from the top part of the nanotube that was broken during sonication. Combining the results from Figure 4a and Figure 4b, it can be concluded that the wall of the resultant nanotubes formed by the spreading of precursor film has a thickness gradient

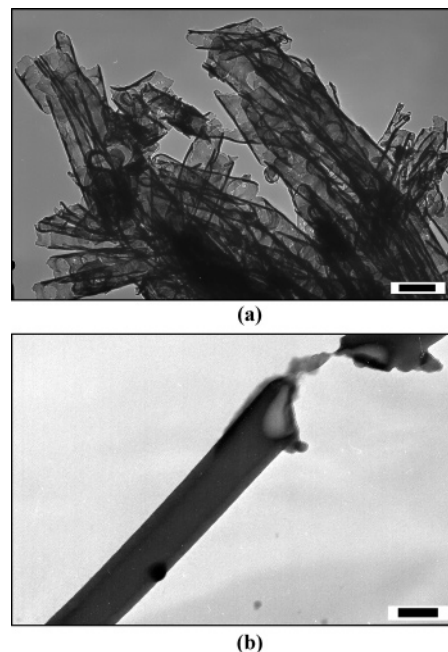


**Figure 4.** TEM images of PS-2 ( $M_n = 83.3$  kg/mol) nanotubes generated within alumina membrane after annealing at 192 °C for 2 h: (a) sample prepared by microtoming (scale bar 500 nm); (b) sample prepared by ultrasonication (scale bar 250 nm). Both samples were stained with RuO<sub>4</sub>.

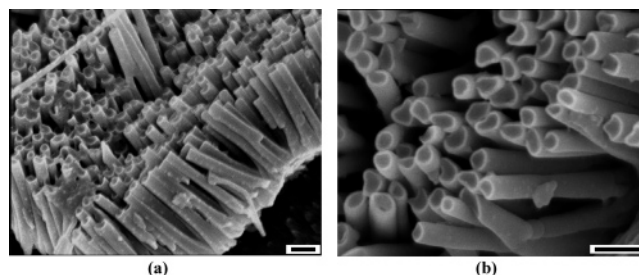


**Figure 5.** SEM images of PS-3 ( $M_p = 760$  kg/mol) nanorods generated within alumina membrane after annealing at 205 °C for 2 h (scale bar 500 nm).

along the nanotube, supporting the SEM observations described above.

The wetting behavior of polystyrenes with ultrahigh molecular weights was also studied. For example, when a polystyrene with the molecular weight of 760 kg/mol (PS-3, peak molecular weight ( $M_p$ ) = 760 kg/mol, PDI < 1.07) was used, even at an annealing temperature of 205 °C, short nanorods were produced, as shown in Figure 5. Again, a meniscus can be clearly seen at the tip of nanorods, indicating that the wetting was driven by capillary force. Obviously, for polystyrene with higher molecular weight, the temperature of wetting transition ( $T_w$ ) is also higher. For PS-3,  $T_w$  is higher than 205 °C.

From the results described above, it is clear that polymers with different molecular weights may have completely different wetting behaviors at the same temperature. For example, at the annealing temperature of 205 °C, complete wetting of alumina membranes occurred when PS-1 ( $M_n = 30.5$  kg/mol) was used, while partial wetting occurred when PS-3 ( $M_p = 760$  kg/mol) was used. Obviously wetting

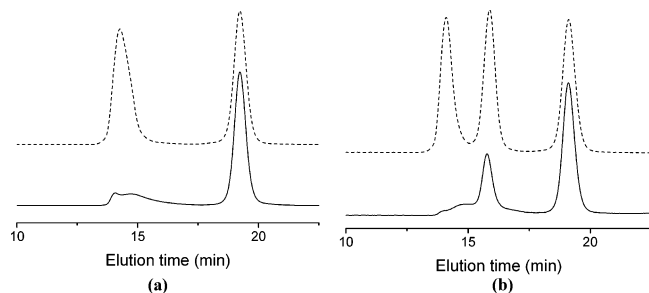


**Figure 6.** SEC traces of the original polystyrene mixtures (dashed line) and the polystyrenes in the resultant nanotubes (solid line) obtained by wetting alumina membranes with melts of polystyrene mixtures at 192 °C for 2 h: (a) polystyrene mixture of PS-1 ( $M_n = 30.5$  kg/mol) and PS-4 ( $M_p = 1,075$  kg/mol) with weight ratio of 1/1; (b) polystyrene mixture of PS-1, PS-4, and PS-5 ( $M_p = 238.7$  kg/mol) with weight ratio of 1/1/1.

through the two mechanisms (capillary force and precursor film) occurs on very different time scales. The wetting by the precursor film is much faster than that driven by the capillary force. This characteristic can be used to fractionate polymers with different molecular weights. For example, when a mixture of two polystyrenes, PS-1 and PS-4 ( $M_p = 1,075$  kg/mol, PDI = 1.05) with the weight ratio of 1/1, was used to wet alumina membranes at 192 °C for 2 h, nanotubes were produced, as indicated by the SEM measurements. Independent experiments under the same annealing condition (192 °C for 2 h) showed that very long nanotubes formed when PS-1 alone was used, while very short nanorods formed when PS-4 was used. One would expect that the nanopores of alumina membranes would be preferentially wetted by the low molecular weight polystyrene (PS-1) when the mixture of PS-1 and PS-4 was used, because of the intrinsic difference in wetting rates between the partial and complete wetting. This is indeed the case. After the alumina membrane was dissolved in NaOH solution, the resultant nanotubes were detached from the supporting bulk film of mixed polystyrenes via ultrasonication in water/ethanol mixture (1/1 in weight). After the removal of the bulk polymer film, the isolated nanotubes were collected on a polycarbonate nucleopore membrane by filtration and then dissolved in THF for the size exclusion chromatography (SEC) measurements. As shown in Figure 6a, in the resultant nanotubes, low molecular weight polystyrene (PS-1) was dominant, as expected. It has to be noted that the bimodal distribution of PS-4 in the resultant nanotubes is due to the fact that the molecular weight of PS-4 is well above the fractionation limit of the SEC columns used (about 400 kg/mol). Similarly, when a ternary mixture of PS-1, PS-4, and PS-5 ( $M_p = 238.7$  kg/mol, PDI = 1.02) was used to wet alumina membrane at 192 °C for 2 h, the low molecular weight polystyrene wetted the alumina nanopores with a much higher rate than those of the high molecular weight ones, as shown in Figure 6b.

In conclusion, during the wetting of nanoporous alumina membranes with polystyrene melts, a transition from the partial to complete wetting was observed when the annealing temperature was raised above a critical temperature  $T_w$ . This

wetting transition is related to the increase of spreading coefficient  $S$  with increasing temperature. The wetting transition temperature ( $T_w$ ) is dependent on the polymer molecular weight. The higher the molecular weight, the higher the  $T_w$ . Thus, tailored polymeric nanostructures (nanorods or nanotubes) can be obtained via wetting alumina membranes with polymer melts simply by controlling the annealing temperature. The large difference in wetting rate between two wetting regimes (partial and complete wetting) was successfully used to fractionate polystyrenes with different molecular weights.

Future work will address the change of the contact angle as a function of annealing temperature to determine the exact wetting transition temperature. The influences of the nature of pore surface and the pore size on the nanopore wetting are also of interest and will be addressed soon.

**Acknowledgment.** This work was supported (J.-T.C., T.P.R.) by the DOE, BES (DE-FG-02-96ER45), the NSF supported Materials Research Science and Engineering Center (P.D.), and the associated Research Experience for Teachers Program (J.O., A.M.) at the University of Massachusetts (DMR 9400488).

**Supporting Information Available:** Detailed experimental procedures for the sample preparation and characterization. This material is available free of charge via the Internet at <http://pubs.acs.org>.

## References

- (1) De Gennes, P. G. *Rev. Mod. Phys.* **1985**, *57*, 827.
- (2) Young, T. *Philos. Trans. R. Soc. London* **1805**, *95*, 65.
- (3) Heslot, F.; Cazabat, A. M.; Levinson, P.; Fraysse, N. *Phys. Rev. Lett.* **1990**, *65*, 599.
- (4) Carles, P.; Troian, S. M.; Cazabat, A. M.; Heslot, F. *J. Phys.: Condens. Matter* **1990**, *2*, SA477.
- (5) Ausserré, D.; Picard, A. M.; Léger, L. *Phys. Rev. Lett.* **1986**, *57*, 2671.
- (6) Léger, L.; Erman, M.; Guinet-Picard, A. M.; Ausserré, D.; Strazielle, G. *Phys. Rev. Lett.* **1988**, *60*, 2390.
- (7) Heslot, F.; Cazabat, A. M.; Levinson, P. *Phys. Rev. Lett.* **1989**, *62*, 1286.
- (8) Heslot, F.; Fraysse, N.; Cazabat, A. M. *Nature* **1989**, *338*, 640.
- (9) Xu, H.; Shirvanyants, D.; Beers, K.; Matyjaszewski, K.; Rubinstein, M.; Sheiko, S. S. *Phys. Rev. Lett.* **2004**, *93*, 206103.
- (10) Moon, S. I.; McCarthy, T. J. *Macromolecules* **2003**, *36*, 4253.
- (11) Steinhart, M.; Wendorff, J. H.; Greiner, A.; Wehrspohn, R. B.; Nielsch, K.; Schilling, J.; Choi, J.; Gösele, U. *Science* **2002**, *296*, 1997.
- (12) Xiang, H.; Shin, K.; Kim, T.; Moon, S. I.; McCarthy, T. J.; Russell, T. P. *Macromolecules* **2004**, *37*, 5660.
- (13) Cahn, J. W. *J. Chem. Phys.* **1977**, *66*, 3667.
- (14) Milchev, A.; Milchev, A.; Binder, K. *Comput. Phys. Commun.* **2002**, *146*, 38.
- (15) Shin, K.; Xiang, H.; Moon, S. I.; Kim, T.; McCarthy, T. J.; Russell, T. P. *Science* **2004**, *306*, 76.
- (16) Xiang, H.; Shin, K.; Kim, T.; Moon, S.; McCarthy, T. J.; Russell, T. P. *J. Polym. Sci., Part B: Polym. Phys.* **2005**, *43*, 3377.
- (17) Xiang, H.; Shin, K.; Kim, T.; Moon, S. I.; McCarthy, T. J.; Russell, T. P. *Macromolecules* **2005**, *38*, 1055.
- (18) Steinhart, M.; Senz, S.; Wehrspohn, R. B.; Gösele, U.; Wendorff, J. H. *Macromolecules* **2003**, *36*, 3646.
- (19) Steinhart, M.; Wehrspohn, R. B.; Gösele, U.; Wendorff, J. H. *Angew. Chem., Int. Ed.* **2004**, *43*, 1334.
- (20) Kim, E.; Xia, Y.; Whitesides, G. M. *Nature* **1995**, *376*, 581.

NL060407N